THE ASTROPHYSICAL JOURNAL, 554:L107–L110, 2001 June 10
© 2001. The American Astronomical Society. All rights reserved. Printed in U.S.A.

DETECTION OF HIGH-LATITUDE WAVES OF SOLAR CORONAL ACTIVITY IN EXTREME-ULTRAVIOLET DATA FROM THE *SOLAR AND HELIOSPHERIC OBSERVATORY* EUV IMAGING TELESCOPE

E. E. BENEVOLENSKAYA,[1,2] A. G. KOSOVICHEV,[2] AND P. H. SCHERRER[2]
Received 2001 March 13; accepted 2001 May 8; published 2001 June 4

ABSTRACT

We present the results of an investigation of EUV coronal structures in 1996–2000 using the *Solar and Heliospheric Observatory* EIT data in 171, 195, 284, and 304 Å lines. During this period, poleward- and equatorward-migrating waves of solar activity have been found in axisymmetrical distributions of EUV intensity in all four lines. In the axisymmetrical distribution of the ratio of 195 Å to 171 Å intensities, which is a proxy of coronal temperature from 1×10^6 to 2×10^6 K, the polar branches are less prominent. The high-latitude activity waves are caused by giant coronal magnetic loops connecting the polar magnetic field (formed during the preceding solar cycle) with the magnetic field of the "following" parts of active regions that emerged during the rising phase of the current cycle. We suggest that these coronal loops play an important role in the topological evolution of the magnetic structure of the Sun during the solar cycle.

Subject headings: Sun: activity — Sun: interior — Sun: magnetic fields — Sun: rotation — sunspots

1. INTRODUCTION

Solar activity is closely related to the evolution of the magnetic field of the Sun. It is assumed that the cyclic behavior of the solar magnetic field is associated with dynamo processes in the solar interior. During a solar magnetic cycle, which typically lasts 22 yr, the magnetic topology changes from a largely poloidal field in the activity minima to a predominantly toroidal field in the maxima. Magnetic polarity of the fields is reversed every 11 yr. The toroidal field forms bipolar active regions and sunspots in low-latitude zones that migrate from approximately 30° latitude toward the equator during the 11 yr sunspot cycles (or magnetic half-cycles), forming the famous "butterfly" diagram.

The topological model of the solar cycle suggested by Babcock (1961) introduced two main elements of the cycle: the generation of the toroidal field by the solar differential rotation from the poloidal field and the regeneration of the poloidal field due to poleward migration of the following magnetic polarities of active regions and reconnection in the corona across the equator. This results in the reversal of the polar field polarities around the sunspot maxima. Following Babcock's ideas, Leighton (1969) and Wang, Sheeley, & Nash (1991) developed quantitative models of the poleward migration due to meridional circulation and diffusion, which can closely reproduce the dynamics of the surface fields by adjusting the speed of meridional circulation and the diffusion coefficient. Theoretical investigations led to a suggestion that the poloidal field is likely to be generated by cyclonic convection ("α-effect") in the convection zone (Parker 1955). This model can also explain the equatorward migration of the magnetic zones ("dynamo waves").

Observations of solar corona and polar prominences (Secchi 1877; Waldmeier 1957) established the existence of a high-latitude counterpart of the butterfly diagram that is formed by migrating polar prominences and may consist of two zones appearing with a 2–3 yr interval. Poleward-migrating zones were also observed in coronal emission (see Rŭsin, Rýbansky, & Minarovjech 1998 for a review). These observations inspired suggestions that the polar waves of activity might be associated with another dynamo wave in the convection zone and that, in fact, the poloidal field is reversed by the α-effect rather than by the surface diffusion (Makarov, Ruzmaikin, & Starchenko 1987; Belvedere, Lanzafame, & Proctor 1991). It has also been found that both low- and high-latitude waves of solar activity may last longer the 11 yr sunspot cycle, forming the so-called "extended solar cycle" (e.g., Altrock 1997).

At present, it is unclear whether the processes in the solar corona simply reflect the evolution of the surface or deep fields or whether they play an active role in the changes of the magnetic topology due to magnetic reconnection. This question is an important key to understanding the solar cycle.

2. EVOLUTION OF SOLAR CORONA IN CYCLE 23

We have used synoptic observations of the solar corona in the EUV from the EUV Imaging Telescope (EIT) on the *Solar and Heliospheric Observatory* (*SOHO*) (Delaboudiniere et al. 1995) to study the evolution of the corona during the transition from solar cycle 22 to cycle 23 and the rising phase of cycle 23 in 1996–2000. The solar images were obtained with four narrow bandpass filters: 171 Å (Fe IX and Fe X), 195 Å (Fe XII), 284 Å (Fe XV), and 304 Å (He II). The Fe IX and Fe X images (171 Å) display unresolved emission that is present over most of the quiet Sun, including coronal holes. The Fe XII images (195 Å) are dominated by the closed magnetic field regions of the Sun. All the hottest active region loops are visible in this wavelength, but they are not as clear as in Fe XV (284 Å) line. The Fe XV images are dominated by the hot loops. The He II images (304 Å) are dominated by the transition region network structures and prominences on the solar limb.

The synoptic maps of EUV images in the three lines of Fe and the He II line (171, 195, 284, and 304 Å) are represented by values of the line intensity centered on the central meridian. The original 1024×1024 pixel images were binned to 512×512 pixels, and then each pixel of the CCD rectangular coordinates was transformed into the Carrington coordinate system. For synoptic purposes, the EIT images of the Sun with four

[1] Pulkovo Astronomical Observatory, St. Petersburg 196140, Russia.
[2] W. W. Hansen Experimental Physics Laboratory, Stanford University, Stanford, CA 94305-4085.

EUV filters are taken typically 4 times a day. However, the data set is not homogeneous; quite often, only one image per day was obtained, and for some days there were no data. Therefore, the synoptic maps were constructed using rather wide longitudinal stripes of 16°, centered on the central meridian for each image. When more than one synoptic image per day was available, the stripes overlapped each other. If an EIT image was missing, we used a wider longitudinal stripe from the previous image to cover the missing values. We have constructed the EUV synoptic map for Carrington rotation from CR 1911 to CR 1967, 1996 June 28–2000 September 30. The resolution of these maps is 1° in both longitude from 0° to 360° and latitude from −83° to 83° (Benevolenskaya et al. 2001).

The synoptic maps reveal nonuniform structure of the EUV corona in both longitude and latitude, reflecting the nonuniform distribution of a large-scale magnetic field. To obtain the latitudinal distribution, we averaged the synoptic maps over longitude and plotted as a function of latitude and time in Figures 1*a*–1*d*. These maps show the evolution of the axisymmetrical component and correspond to the well-known butterfly sunspot diagram.

For comparison, we plotted the azimuthally averaged distributions of the unsigned (absolute) magnetic flux $|B_{\|}|$ (Fig. 1*e*) and the line-of-sight magnetic flux $B_{\|}$ (Fig. 1*f*) obtained from the Kitt Peak Observatory synoptic magnetic maps. The dashed curves show the location of the magnetic neutral line separating magnetic polarities at high latitudes. The $|B_{\|}|$ map, which basically shows the location of sunspots and active regions, reveals the familiar butterfly diagram: the sunspot zones of the current solar cycle start at about 30° latitude in mid-1997 and then gradually migrate toward the equator as the cycle progresses. The $B_{\|}$ map reflects the evolution of the large-scale fields and shows a gradual migration toward the poles of the magnetic neutral lines in both hemispheres. These neutral lines separate the polar magnetic field formed during the previous solar cycle from the magnetic field emerging during the current cycle. When the neutral lines reach the poles (usually around the sunspot maxima), this results in a magnetic polarity reversal at the poles.

In the coronal EUV maps, we see in each hemisphere two sets of migrating structures: low-latitude structures that migrate toward the equator following $|B_{\|}|$ and high-latitude structures that migrate toward the poles parallel to the magnetic neutral lines. However, these coronal structures are located 15°–20° higher in latitude than the neutral line. In the EUV data, the polar branches of coronal activity started in 1997 almost simultaneously with the equatorial branch and reached the lower and upper boundaries of our synoptic maps ($\pm 83°$) in early 2000. The polar branches are easily identified in 304, 171, and 195 Å maps.

Figure 2 shows the synoptic map for the ratio of 195 Å to 171 Å emissions. This ratio is mostly sensitive to temperature variations up to 2×10^6 K because both emissions come from the same atomic element (Fe). The polar branches on this map are not as prominent as they are on the intensity maps (Figs. 1*a*–1*d*). This suggests that the polar branches represent coronal structures of enhanced plasma density. Using the EIT calibration software, we have estimated the differential emission measure and coronal temperature from I_{171} and I_{195}. The latitudinal distributions of these properties averaged over several Carrington rotations are presented in Figures 3*a*–3*e* (panel *e* represents results for only one rotation because of an interruption of the *SOHO* observations). Both the differential emission measure and temperature curves clearly show poleward migration of the high-latitude peaks. Evidently, the temperature increase is quite moderate; how-

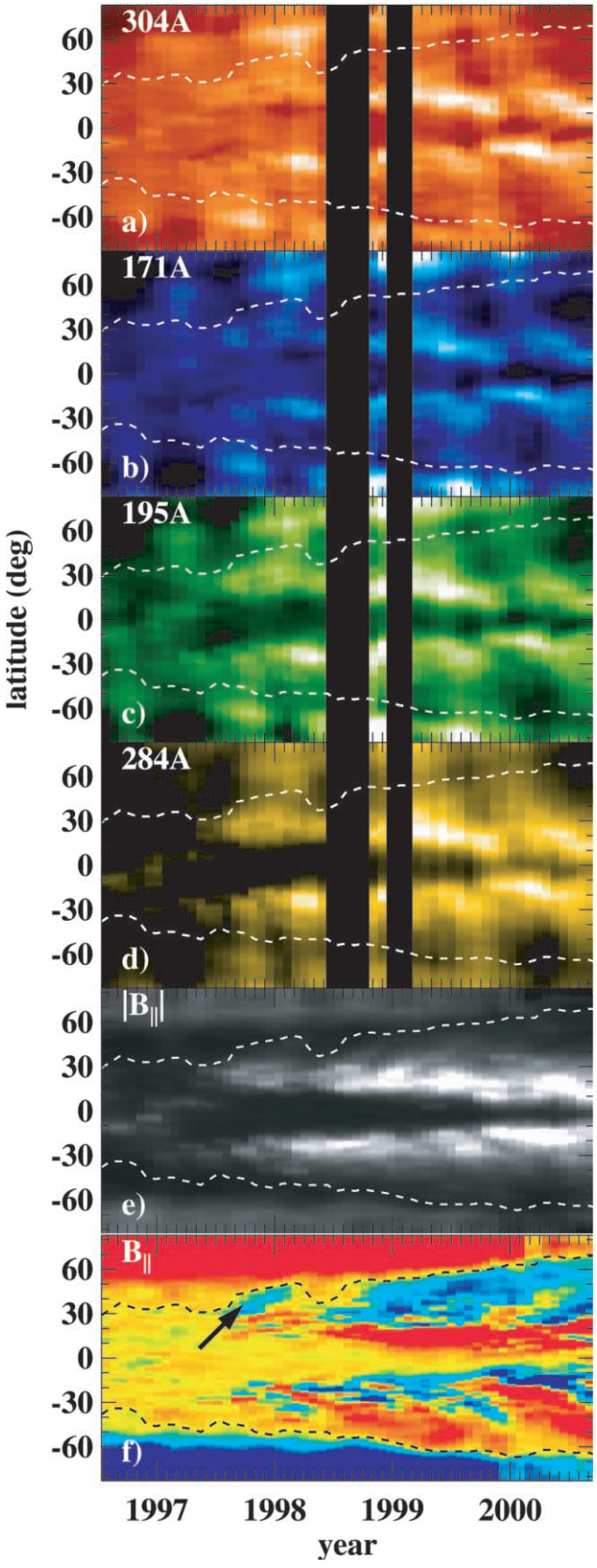

FIG. 1.—Azimuthally averaged intensity of the solar corona as a function of latitude and time in the EUV lines: (*a*) 304 Å, (*b*) 171 Å, (*c*) 195 Å, and (*d*) 284 Å, and the corresponding line-of-sight photospheric magnetic field values: (*e*) $|B_{\|}|$ and (*f*) $B_{\|}$ (red shows the field of the positive polarity, and blue the negative polarity). The dashed curves show the high-latitude magnetic neutral lines.

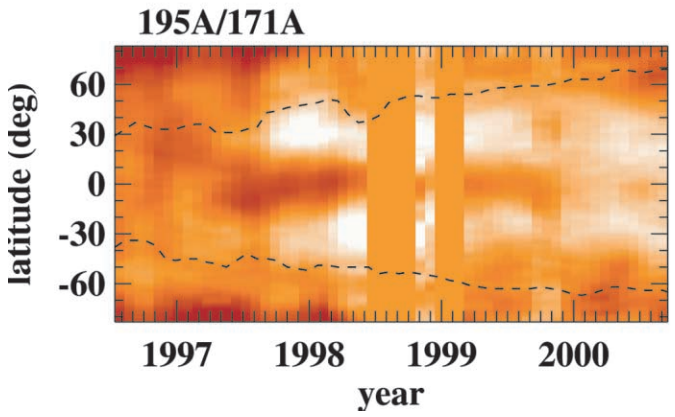

FIG. 2.—Azimuthally averaged temperature-sensitive ratio of 195 Å to 171 Å EUV intensities as a function of latitude and time. The dashed curves show the high-latitude magnetic neutral lines.

ever, when the coronal wave reached the near polar regions, it resulted in a higher plasma temperature in these regions (Fig. 3*e*). This phenomenon may be related to the sudden increase of the coronal temperature near the poles that was observed prior to the previous solar maximum in 1989 by Altrock (1998) and Penn et al. (1998).

3. THE PHYSICAL NATURE OF THE CORONAL HIGH-LATITUDE WAVES

During the 20 months presented in Figure 3, the high-latitude waves migrated from ~55°–60° to ~70°–75°. This corresponds to a mean speed of 3–5 m s^{-1}. The comparison of the EUV intensity diagrams (Figs. 1*a*–1*d*) with the magnetic field diagram (Fig. 1*f*) shows a close correlation between the equatorward boundary of the enhanced coronal emission associated with the high-latitude activity waves and the magnetic neutral line. In one example, at the end of 1997 and beginning of 1998, in Figure 1*f* we can see a large blue region of negative polarity (indicated by an arrow) migrating from 30° to 50°. This process was accompanied by a displacement of the neutral line toward the north pole and by an increase in intensity of the high-latitude wave. This suggests that the high-latitude activity waves are closely related to the magnetic evolution of the Sun and, in particular, to polar field polarity reversal.

The coronal structures associated with the high-latitude waves are easily identified on the EUV synoptic charts as longitudinally extended bright structures at 50°–70° latitude. As an example, Figure 4*a* shows the synoptic map for Carrington rotation 1929 (1997 November 1–28) for the 171 Å line, and Figure 4*b* shows the corresponding magnetic field map. Evidently, the coronal structures appear poleward of the magnetic neutral lines separating magnetic fields of the following polarities from the polar magnetic field.

On the solar limb, these structures are seen as giant loops connecting the following parts of active regions with the polar regions. These limb loops are better seen in the 284 Å line. Figure 5*a* shows a 284 Å image taken during the Carrington rotation 1929, on 1997 November 19. The limb coordinates of this image are shown in the Carrington map (Fig. 4) by two vertical dashed lines. The arrows in both figures point to the same structures (labeled A, B, C, and D), which are evidently the poleward footpoints of the giant loops. Quite often, these loops had low-altitude dark structures in the middle. These dark structures probably correspond to "polar crown prominences"

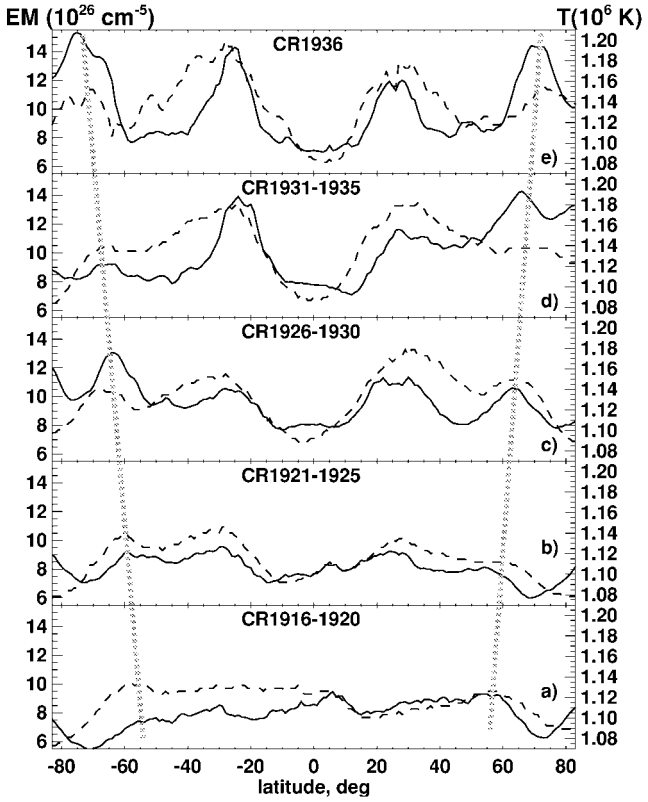

FIG. 3.—Differential emission measure (EM; *solid curves*) and coronal temperature (*T*; *dashed curves*) estimated from 171 and 195 Å intensity data as a function of latitude averaged over several Carrington rotations: (*a*) CR 1916–1920 (1996 November 11–1997 March 28), (*b*) CR 1921–1925 (1997 March 28–August 11), (*c*) CR 1926–1930 (1997 August 11–December 26), (*d*) CR 1931–1935 (1997 December 26–1998 May 11), and (*e*) CR 1936 (1998 May 11–June 7). The vertical dotted gray lines trace the high-latitude maxima associated with the coronal activity waves.

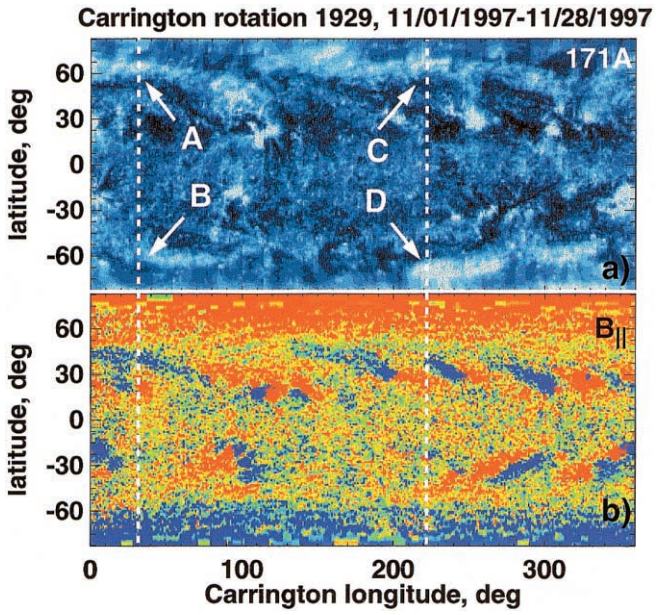

FIG. 4.—(*a*) EIT 171 Å intensity map for CR 1929 (1997 November 1–28). (*b*) Corresponding magnetic field map (red shows the field of positive polarity, blue the negative polarity). The dashed vertical lines indicate the positions of the solar limb of the EIT image of 1997 November 19, which is shown in Fig. 5*a*. The arrows indicate the features (A–D) corresponding to loop structures in the 1997 November 19 image.

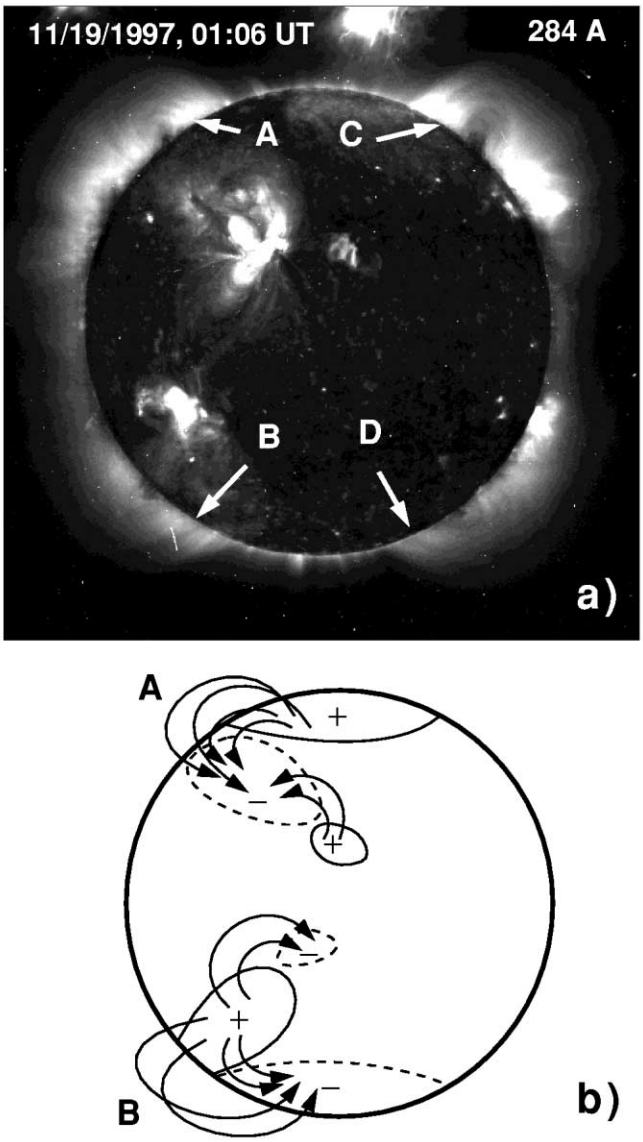

FIG. 5.—(*a*) EIT image in 284 Å line on 1997 November 19, 01:06 UT. The arrows identify the looplike structures (A–D) that are parts of the longitudinally extended high-latitude structures visible in Fig. 4*a*. (*b*) Schematic picture showing the magnetic connections between the leading and following polarities of active regions and the polar field.

located at the magnetic neutral lines, which normally have "coronal cavities" surrounding them.

Therefore, the high-latitude waves of activity migrating poleward, as revealed by the coronal butterfly-type diagrams, are formed by longitudinally extended magnetic arcades connecting the following parts of active regions with the polar regions.

4. CONCLUSION

We conclude that the bright coronal structures detected in the EUV data from *SOHO*/EIT, which migrated to the poles during the rising phase of the solar cycle, were formed by density enhancements in the poleward footpoints of magnetic field lines connecting the magnetic fields of the following parts of active regions with the polar field. These magnetic connections are illustrated in Figure 5*b*. The high-latitude coronal structures connect the predominantly poloidal polar magnetic field, formed during the preceding solar cycle, with the magnetic field of active regions, which emerged during the current cycle and is mostly toroidal. These magnetic connections are probably formed by reconnection processes in the corona at the beginning of the current cycle in 1997–1998 as indicated by enhancements in the coronal temperature in Figure 3. However, direct evidence for the reconnection has not been obtained; this is a subject of further investigation. Our results suggest that the coronal connections between the polar poloidal field formed during the preceding cycle and the toroidal field of the new cycle are likely to play a significant role in the topological evolution of the solar magnetic field with the activity cycle.

We thank the anonymous referee for useful comments. This work was partly supported by a NASA JURRISS grant and the SOI/*SOHO* NASA contract NAG5-8878 to Stanford University. *SOHO* is a project of international cooperation between ESA and NASA.

REFERENCES

Altrock, R. C. 1997, Sol. Phys., 170, 411
———. 1998, in ASP Conf. Ser. 140, Synoptic Solar Physics, ed. K. S. Balasubramaniam, J. W. Harvey, & D. M. Rabin (San Francisco: ASP), 339
Babcock, H. M. 1961, ApJ, 133, 572
Belvedere, G., Lanzafame, G., & Proctor, M. R. E. 1991, Nature, 350, 481
Benevolenskaya, E. E., Kosovichev, A. G., Scherrer, P. H., & Lemen, J. 2001, Sol. Phys., submitted
Delaboudiniere, J.-P., et al. 1995, Sol. Phys., 162, 291
Leighton, R. B. 1969, ApJ, 156, 1
Makarov, V. I., Ruzmaikin, A. A., & Starchenko, S. V. 1987, Sol. Phys., 111, 267
Parker, E. N. 1955, ApJ, 122, 293
Penn, M., Altrock, R. C., Henry, T., & Gahathakurta, M. 1998, in ASP Conf. Ser. 140, Synoptic Solar Physics, ed. K. S. Balasubramaniam, J. W. Harvey, & D. M. Rabin (San Francisco: ASP), 325
Rŭsin, V., Rýbansky, M., & Minarovjech, M. 1998, in ASP Conf. Ser. 140, Synoptic Solar Physics, ed. K. S. Balasubramaniam, J. W. Harvey, & D. M. Rabin (San Francisco: ASP), 353
Secchi, P. A. 1877, Le Soleil, Vol. 2 (Paris: Gauthier-Villars)
Waldmeier, M. 1957, Die Sonnenkorona, Vol. 2 (Basel: Birkäuser)
Wang, Y.-M., Sheeley, N. R., & Nash, A. G. 1991, ApJ, 383, 431